CD96 Interaction with CD155 via Its First Ig-like Domain Is Modulated by Alternative Splicing or Mutations in Distal Ig-like Domains*S

Received for publication, October 6, 2008 Published, JBC Papers in Press, December 4, 2008, DOI 10.1074/jbc.M807698200

Dorothee Meyer^{‡1}, Sebastian Seth^{‡1,2}, Jana Albrecht[‡], Michael K. Maier[‡], Louis du Pasquier[§], Inga Ravens[‡], Lutz Dreyer[‡], Renate Burger[¶], Martin Gramatzki[¶], Reinhard Schwinzer[|], Elisabeth Kremmer^{**}, Reinhold Foerster[‡], and Günter Bernhardt^{‡3}

From the † Institute of Immunology and the $^{\parallel}$ Transplantation Laboratory, Department of Visceral and Transplantation Surgery, Hannover Medical School, Carl-Neuberg Strasse 1, 30625 Hannover, Germany, the § Institute of Zoology, and Evolutionary Biology, University of Basel, Vesalgasse 1, Basel, CH 4051, Switzerland, the Division of Stem Cell Transplantation and Immunotherapy, Second Department of Medicine, University Medical Center SH Campus Kiel, Schittenhelmstrasse 12, 24105 Kiel, Germany, and the **Institute of Molecular Immunology, Helmholtz Zentrum München, Marchioninistrasse 25, 81377 Munich, Germany

The adhesion receptor CD96 (TACTILE) is a transmembrane glycoprotein possessing three extracellular immunoglobulinlike domains. Among peripheral blood cells, CD96 is expressed on T cells as well as NK cells and a subpopulation of B cells. A possible function of this receptor in NK cell-mediated killing activities was suggested recently. Moreover, CD96 was described as a tumor marker for T-cell acute lymphoblastic leukemia and acute myeloid leukemia. CD96 binds to CD155 (poliovirus receptor) and nectin-1, an adhesion receptor related to CD155. Here we report that human but not mouse CD96 is expressed in two splice variants possessing either an I-like (variant 1) or V-like (variant 2) second domain. With the notable exception of an AML tumor sample, variant 2 predominates in all the CD96-expressing cell types and tissues examined. Using chimeric human/murine CD96 receptors, we show that the interaction with its ligands is mediated via the outermost V-like domain. In contrast to mouse, however, the binding of human CD96 to CD155 is sensitive to the characteristics of the two downstream domains. This is illustrated by a significantly weaker CD96/CD155 interaction mediated by variant 1 when compared with variant 2. Moreover, recent evidence suggested that mutations in human CD96 correlate with the occurrence of a rare form of trigonocephaly. One such mutation causing a single amino acid exchange in the third domain of human CD96 decreased the capacity of both variants to bind to CD155 considerably, suggesting that a CD96-driven adhesion to CD155 may be crucial in developmental processes.

CD96 is a single pass transmembrane glycoprotein belonging to the Ig superfamily (1). In its extracellular part, CD96 consists of three Ig-like domains in the order $V_{N-\mathrm{term}}$ -V- $C_{C-\mathrm{term}}$ and a membrane proximal region rich in proline/serine/threonine. It is assumed that extensive O-linked glycomodification of this region equips CD96 with a semi-flexible stalk. Therefore, the Ig-like domains may protrude among other membrane-bound macromolecules comprising the outer layer of the cell (1). Even though such exposed presentation predestines CD96 for roles in adhesion, interaction partners of CD96 as well as its biological function(s) remained largely obscure until recently. However, CD96 was described as tumor marker for T-ALL and AML characteristic for the AML stem cell in particular (2, 3). Among human peripheral blood cells, CD96 expression was observed on T and NK cells but not on the majority of B cells, monocytes, and granulocytes (4). The murine CD96, characterized recently, is widely expressed on T cells of all developmental and differentiation stages tested albeit to varying extents (5). This is in line with the original observation of elevated CD96 expression in activated human T cells (1).

In humans, CD96 promotes adhesion of NK cells to tumor cells expressing CD155, an interaction that may assist in NKmediated destruction of the targets (4); yet direct evidence proving CD96 as NK receptor is missing. Although CD155 remained the only identified interaction partner for CD96 in human (4), nectin-1 also binds to CD96 in mouse (5). Although the significance of the CD96/nectin-1 interaction remains unclear, it is interesting to note that nectin-1 is expressed prominently in brain and, in particular, localizes to the synaptic junctions. Nectin-1-deficient mice suffer from microphthalmia (small eyes), an eye disorder caused by malformation of cell layers of the ciliary epithelia (6). In humans, mutations in nectin-1 were associated with the occurrence of cleft lip/palateectodermal dysplasia syndrome (7), whereas a mutation in CD96 (T280M) or disruption of the genetic locus of CD96 by chromosomal translocation link to a distinct manifestation of the C syndrome (Opitz Trigonocephaly) (8). Nectin-1 as well as CD155 belong to a subfamily of Ig-like adhesive receptors (9). An evolutionary analysis revealed that the members of this family share a common progenitor with CD96 and CD226 (10),



^{*} This work was funded by Deutsche Forschungsgemeinschaft Grant BE1886/ 2-1 (to G.B.). The costs of publication of this article were defrayed in part by the payment of page charges. This article must therefore be hereby marked "advertisement" in accordance with 18 U.S.C. Section 1734 solely to indicate this fact.

The on-line version of this article (available at http://www.jbc.org) contains supplemental Fig. S1.

¹ These authors contributed equally to this work.

² Recipient of a Georg Christoph Lichtenberg Stipend provided by the Ph. D. program Infection Biology sponsored by the Ministry of Science and Culture of Lower Saxony.

³ To whom correspondence should be addressed: Institute of Immunology, Hannover Medical School, Carl-Neuberg Str. 1, 30625 Hannover, Germany. Fax: 49-511-532-9722; E-mail: bernhardt.guenter@mh-hannover.de.

another binding partner for CD155 (11). Mice deficient for CD155 produce a reduced humoral immune response to soluble antigens entering the organism via the gastrointestinal tract, whereas subcutaneous or systemic immunizations are not affected (12). These findings document the involvement of CD96 and members of the CD155/nectin family in immunological as well as developmental processes.

In this study we were interested to investigate the interaction of CD96 with its binding partners in more detail. To this end, chimeric receptors were generated consisting of distinct mouse and human Ig-like domains. It could be demonstrated that the first domain of CD96 harbors the epitope(s) essentially required for CD155 binding. However, the magnitude of binding is modulated by the second domain in case of human but not mouse CD96. Contrary to murine CD96, human CD96 is alternatively spliced, giving rise to two isoforms differing in the Ig fold of the second domain. Expression analysis by real time PCR revealed that the shorter variant is predominantly expressed in all nonmalignant tissue and cell types investigated. CD155 binds to both splice variants yet with different strength. Moreover, the T280M mutation residing in Ig-like domain three of CD96 resulted in a significantly reduced binding to CD155.

EXPERIMENTAL PROCEDURES

Cloning of Human CD96 cDNA—Full-length hCD96⁴ was cloned out of white blood cell cDNA (Clontech) by PCR (Expand high fidelity; Roche Applied Science). The cycling conditions were: 1 min at 94 °C, then 10 cycles consisting of 15 s at 94 °C, 30 s at 55 °C, 2 min at 72 °C, and an additional 15 cycles of 15 s at 94 °C, 30 s at 55 °C, 2 min at 72 °C with an extension time of 5 s/cycle. The primers used were: HCD96.KPN, 5′-GCG GTA CCG GTG TTC AGA AGA CAA TGG AG-3′; and hcd96_xba, 5′-GCT CTA GAC TAG AGG GTC TCC ATC TCA TGA T-3′.

After cloning into pcDNA3, the products were sequenced. Two types of cDNA inserts were obtained (see also Ensembl data base entry ENSG00000153283). Variant 1 (hCD96V1) represents the hCD96 version carrying exon 4, whereas in variant 2 (hCD96V2) this exon is missing, causing the absence of 18 amino acids. Exon 4 borders are in frame (phase 0) such that differential splicing does not cause additional amino acid changes.

Detection of hCD96 Proteins by Western Blotting—To visualize hCD96 proteins, the pCDNA3 plasmids driving the expression of murine ICAM-1, hCD96V1 or hCD96V2 were transiently transfected into HEK293 cells (see below). After 2 days the cells were surface-biotinylated. The AML cell line KG1 endogenously expressing hCD96 served as a positive control. For biotinylation, $\sim\!5\times10^7$ cells were detached with PBSd, 10 mM glucose/2 mM EDTA (only for HEK293) and washed twice with PBSd, 10 mM glucose and resuspended in 1 ml of PBSd, 10

mm glucose. 2 mg of biotinylation reagent (No-weigh NHS-PEO4-Biotin; Thermo Scientific) was dissolved in 1 ml of PBSd, 10 mm glucose and added to the cells. The mixture was slowly rotated at room temperature for 30 min and then washed twice with 15 ml of PBSd, 10 mM glucose. The pellet was resuspended in 1 ml of PBSd, 0.25% Nonidet P-40, incubated for 20 min on ice, and centrifuged to obtain cell extract. For immunoprecipitations, the cell extracts were rocked gently either with 10 μ g of anti-hCD96 antibody TH-111 (2) or 20 µg of recombinant hCD155-hIgG protein along with 25 μl of protein G-Sepharose beads (GE Healthcare) overnight at 4 °C. The beads were then washed twice with PBSd, 0.25% Nonidet P-40 and twice with PBSd. The beads were boiled in 30 µl of Laemmli buffer. Following SDS-PAGE on a 10% BisTris gel (Invitrogen), the proteins were blotted, and the biotinylated material was revealed after blocking with dry milk in TBST and incubation/detection with streptavidin-alkaline phosphatase (Sigma) and nitro blue tetrazolium/5-bromo-4-chloro-3-indolyl phosphate.

Construction of Chimeric and Mutant Receptors-Fulllength cDNAs coding for hCD96V2 and mCD96 were subjected to site-directed mutagenesis to create ClaI or BlpI sites according to the manufacturer's instruction (Stratagene). Although the introduction of the BlpI site was silent, that of the ClaI site caused one amino acid substitution (hCD96, A142T; mCD96, Q141T). Domain interchanges were done applying appropriate restriction enzyme digests. The T280M mutation was inserted into both hCD96 cDNA versions. All of the mutant clones were sequenced to verify their integrity. The primers used were: HCD96D12, 5'-CAT TCA GAC ACA CGT TAC AAT CGA TGA ATG GAA CAG CAA CC; hcd96_d125'-GGT TGC TGT TCC ATT CAT CGA TTG TAA CGT GTG TCT GAA TG; HMCD96D23, 5'-TCC ACC ACA GTC AAG GTT TTT GCT AAG CCA GAA ATC C; hmcd96_d23, 5'-GGA TTT CTG GCT TAG CAA AAA CCT TGA CTG TGG TGG A; MUCD96D12, 5'-CAT TGT GGA ACC CTA TAC AAT CGA TGA ACA CAA CTA TAC AAT AG; mucd96_d12, 5'-CTA TTG TAT AGT TGT GTT CAT CGA TTG TAT AGG GTT CCA CAA TG; CD96T280M, 5'-GTG ATT GTG GAA AAT AAC TCC ATG GAT GTC TTG GTA G; and cd96 t280m, 5'-CTA CCA AGA CAT CCA TGG AGT TAT TTT CCA CAA

Transient Transfection and Binding of Antibodies or Recombinant Proteins—Twenty μg of cDNA encoding the diverse human/murine CD96 versions were transfected into HEK293 cells along with 2 μg of a green fluorescent protein-expressing plasmid applying the standard calcium phosphate transfection technique. The cells were detached 48 h later and incubated with either anti-hCD96 antibody TH-111 or a panel of anti-mCD96 antibodies clones 6A6, 8B10, or 6B4, respectively (see Ref. 5 for details). Rat anti-mouse IgG-Cy5 or mouse anti-rat IgG-Cy5 secondary antibodies were used for detection.

CD155 and nectin-1 were expressed and purified as recombinant hIgG1 proteins as described earlier (5). They consist of the entire ectodomain of CD155 or nectin fused to domains 3 \pm 4 of hIgG1. Transfected cells were first incubated with 2 μg of recombinant protein on ice and washed twice, and bound protein was detected by mouse anti-human biotin/streptavidin PerCP.



⁴ The abbreviations used are: hCD, human CD; mCD, murine CD; mAb, monoclonal antibody; BisTris, 2-[bis(2-hydroxyethyl)amino]-2-(hydroxymethyl)-propane-1,3-diol; EYFP, enhanced yellow fluorescent protein; T-ALL, T-cell acute lymphoblastic leukemia; AML, acute myeloid leukemia; PBSd, PBS deficient in Ca²⁺ and Mg²⁺.

For titration of recombinant protein on HEK293 cells transiently expressing hCD96V1, hCD96V1m, hCD96V2, or hCD96V2m, respectively, the cells were incubated with the indicated amounts of recombinant hCD155-hIgG1 in 50 µl of PBSd, 2% fetal calf serum for 1 h on ice. After three washes bound protein was detected using goat anti-hIgG-bio/streptavidin Cy5. In parallel samples, the cells were incubated with decreasing amounts of mAb TH-111 and washed, and bound mAb revealed by adding rat anti-mouse IgG-Cy5. For flow cytometry, propidium iodide was added to exclude dead cells from analysis. The cells were analyzed on a FACSCalibur or LSRII (BD Biosciences), and the data were evaluated using WinList5.0.

The binding of mAb and recombinant protein (as seen in Fig. 3) was normalized to cover a range from 0 to 100, where 100 was assigned to the binding to the parental receptors (hhh in case of TH-111 and hCD155-IgG; mmm for 6A6, 8B10, 6B4, and mCD155-IgG, respectively) using the following formula.

$$relative \ binding = \frac{linMeanX - linMeanX_{base \ line}}{linMeanX_{physiological} - linMeanX_{base \ line}} \cdot 100$$

(Eq. 1)

Three independent experiments were included in the analysis, allowing the calculation of the mean and S.D. for representa-

The TH-111 binding efficiencies to different hCD96 variants (Fig. 4) were determined by titration. The linMeanX values were normalized for plotting using the following formula.

normalized mAb binding

$$= \frac{\textit{linMeanX}_{\text{sample}} - \textit{linMeanX}_{\text{base line}}}{\textit{linMeanX}_{\text{max}} - \textit{linMeanX}_{\text{base line}}} \cdot 100 \quad \text{(Eq. 2)}$$

Signals detected from protein binding were corrected to include the expression level of each CD96 variant by dividing by the half-maximal signal of mAb TH-111.

corrected binding =
$$\frac{linMeanX (CD155)}{linMeanX_{50} (TH-111)}$$
 (Eq. 3)

The results were then normalized to a scale from 0 to 100, thereby adjusting the strongest binding (elicited by hCD96V2 binding to the highest amount of hCD155-IgG) to 100. Three independent experiments were included in the analysis, allowing the calculation of the mean and S.D. for representation.

Electroporation of Raji Cells and Cell Adhesion Assay—Raji cells were grown in RPMI 1640, 10% fetal calf serum and taken up at 2×10^7 cells/ml in growth medium following centrifugation. 400 µl of cells were mixed in a cuvette (0.4 cm electrode gap) with $10-20 \mu g$ of expression plasmid, $10 \mu l$ of 0.2 M ATP, and 3 µl of 1 M MgCl₂. Electroporation was done at 240 V and 1,500 microfarad. The cells were then kept for 2 days in growth medium.

For cell adhesion assays, EYFP-tagged hCD96 receptors were constructed. First, the XbaI fragment of vector pEYFP (Clontech) containing the open reading frame for the fluorescent protein EYFP was cloned into pCDNA3 (Invitrogen) to yield

vector pCDNA3-EYFP. Next, hCD96 fusion fragments encompassing the entire ectodomain of either hCD96 variant were generated by PCR for in frame cloning into the BamHI site of pCDNA3-EYFP. PCR conditions were as described above with the full-length hCD96 clones as templates using the following primers: HSCD96.BAM, 5'-GCG GAT CCG GTG TTC AGA AGA CAA TGG AG; and hscd96 bamfus, 5'-GCG GAT CCA GGG TCT CCA TCT CAT GAT AAG G. The correct sequences of the fusion clones, hCD96V1-EYFP and hCD96V2-EYFP, was verified by sequencing. Expression of the fusion proteins following transfection into HEK293 cells confirmed that EYFP fluorescence linearly increased with the amount of bound anti-hCD96 antibody, thus providing a tool for monitoring expression efficiency (not shown).

96-well plates were coated with 1 μ g/100 μ l of PBSd/well of recombinant hCD155-hIgG or murine nectin-2-hIgG protein overnight at 4 °C. The wells were washed with RPMI 1640, 10% fetal calf serum before 2×10^6 Raji cells in $\sim 200 \mu l$ of growth medium/well, transiently expressing equal percentages, and amounts of hCD96 fusion receptors were seeded into 96-well plates in triplicate. Raji cells expressing cytosolic EYFP following transfection of vector pCDNA3-EYFP served as controls. The plates were then spun shortly and incubated for 90 min. at 37 °C. Unbound cells were then removed by two washing steps using 200 μ l of growth medium. The attached cells were quantified using the CellTiter96 nonradioactive cell proliferation assay (Promega) according to the instructions of the manufacturer.

Isolation of Primary Human Cells, RNA Preparation, and Real Time PCR—White blood cells from healthy donors were prepared using a Biocoll (Biochrom) gradient. The obtained cells from 40 ml of blood were MACS sorted using the CD56 MultiSort kit (Miltenyi), and the CD56⁺ cell population was stained with mouse anti-hCD3-PerCP (BD Biosciences) to sort out CD3⁻ NK cells on a FACSAria (BD Biosciences). The CD3⁺ CD4⁺ and CD3⁺ CD8⁺ subpopulations were isolated accordingly from human blood following MACS separation of CD3⁺ cells with CD3 MicroBeads (Miltenyi) and subsequent staining with anti-CD4/anti-CD8 mAb (in-house preparations) and flow cytometric separation. Monocytes and B cells were obtained as CD14⁺ and CD20⁺ fractions following MACS separation. The purity (>95%) of all isolated populations was confirmed by reanalysis.

Total RNA was prepared using the Absolutely RNA Microprep Kit (Stratagene). RNA was reverse transcribed (Superscript II reverse transcriptase; Invitrogen) using random hexamer primers. For other human fetal and adult tissues, premade template cDNAs were used (human MTC panel II, human immune system MTC panel, and human fetal MTC panel; Clontech). The ages of the spontaneously aborted fetuses were: 20-33 weeks (fetal brain), 16-32 weeks (fetal spleen), 21-37 weeks (fetal kidney), and 16-32 weeks (fetal thymus). cDNA samples representing AML and T-ALL (13) were obtained from Dr. J. Krauter (Hannover Medical School) and Dr. M. Stanulla (Hannover Medical School). The expression of hypoxanthine phosphoribosyl transferase, hCD96V1, and hCD96V2 was analyzed using a Lightcycler 2.0 (Roche Applied Science) and the Fast Start DNA Master plus SYBR Green Kit (Roche Applied



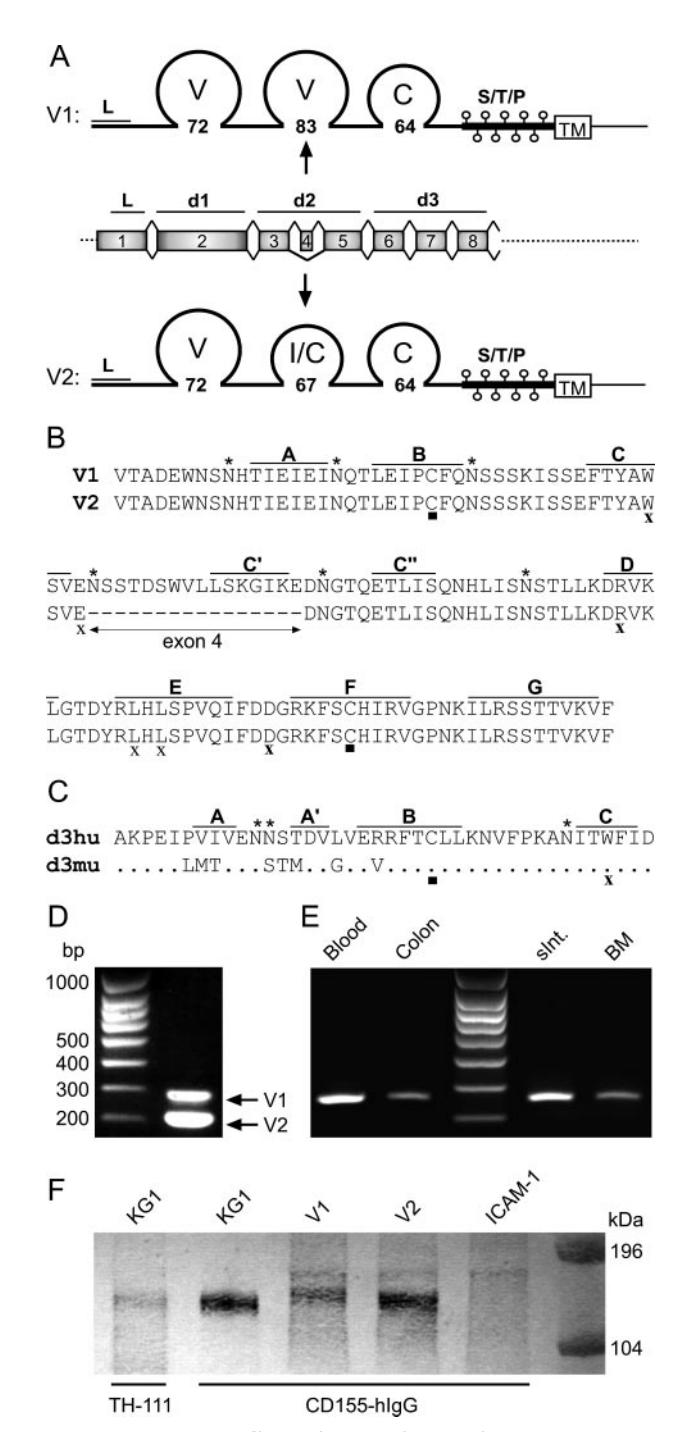


FIGURE 1. Human CD96 splice variants. A, shown is the exon composition of the CD96 gene with respect to the extracellular Ig-like domains. The presence or absence of exon 4 in the mature mRNA results in CD96 isoforms possessing either a V-like or an I/C-like second domain. The numbers in the circles denote the linear distance of the two cysteine residues forming the intradomain disulfide bridge. The membrane-proximal domain representing the S/T/Prich stalk is in bold face where lollipops indicate O-linked disaccharides. L, putative leader sequence; TM, the transmembrane domain. V1, hCD96V1; V2, hCD96V2. B, the amino acid sequence coding the second domain with the predicted β -strand assignment (A, B, C, C', C'', D, E, F, and G) is given. The dashes indicate the locations of those amino acids absent in V2 compared with V1. Diagnostic residues serving as landmarks for the lg fold are indicated as black boxes (cysteine forming intradomain disulfide bridge), as bold face or regular x in case of very well or less well conserved amino acids, respectively. Asterisks indicate N-linked glycosylation sites. C, the sequences comprising the beginning of the third domain of human (d3hu) and murine (d3mu) CD96 are aligned. Dots indicate an identical amino acid in mouse. D, reverse transcription-PCR detecting hCD96 expressed by the human AML cell line KG1.

Science) or the Sybr Premix Ex Taq Kit (Takara). Standardization and absolute relative quantification of expression levels was done as described (14). hCD96 primer combinations used were RTPC96UP/rtpc96_ex4 to detect hCD96V1 and RTPC96UP/rtpc96_alt35 for hCD96V2. Both PCR products were cloned, and the inserts were verified by sequencing. These plasmids were then applied as internal standards and also used to demonstrate that the hCD96V1 specifying primer set did not yield any signal on the hCD96V2 template and vice versa. The primers used were: RTPCD96UP, 5'-AAC AGC AAC CAT ACG ATA GAA ATA GA; rtpcd96_alt35, 5'-TTC CAT TAT CCT CCA CCG ACC; and rtpcd96_ex4, 5'-CTT AGA AAG AAG GAC CCA AGA ATC.

Ig Folding Prediction and β -Strand Assignment—The sequences representing the Ig-like domains of CD96 were sent to the PHYRE server of the Imperial College (London, UK) and to the Jpred server of the Barton group, University of Dundee for secondary structure predictions.

RESULTS

Human CD96 Exists in Two Splice Variants Affecting the Ig Fold of the Second Domain-When cloning human CD96, we noticed a PCR product that represented a version of CD96 lacking exon 4 (Fig. 1, A and D). This exon is 48 nucleotides in length, preserves the open reading frame when spliced out, and maps to the second Ig-like domain (Fig. 1, A and B). A closer analysis involving strand prediction using two different programs suggests that this Ig-like domain belongs to the V-like subset when containing exon 4 amino acids (hCD96V1), whereas the domain encoded by mRNA lacking exon 4 adopts features resembling an I- or a C-like domain, despite maintaining a V-like core folding pattern (hCD96V2). Notably, we failed to identify the corresponding splice variants in mouse. Alignments suggest that murine CD96 is equivalent to human variant 2 (i.e. the short one). Attempts to detect a putative variant 1 by PCR applied on several murine organ cDNAs were unsuccessful (Fig. 1, compare D and E). This observation is fitting with the exon/intron organization of the mouse gene that does not offer the equivalent of the short human exon 4 in this region of the gene (not shown).

Flow cytometry revealed that CD96 is expressed by the human AML cell line KG1. Therefore, KG1 cells were surface-biotinylated and subjected to immunoprecipitations to visualize hCD96 by SDS-PAGE/Western blotting (Fig. 1*F*). Both the anti-hCD96 mAb TH-111 as well as recombinant hCD155-hIgG, precipitated a protein with an apparent molecular weight

Arrows indicate the diagnostic fragments indicative for V1 and V2. *E*, reverse transcription-PCR detecting mCD96 expressed by various murine tissues. The PCR product represents a homolog to V2, a band revealing a putative V1 homolog migrating at a slightly higher position is missing. *F*, immunoprecipitations detecting hCD96 variants. The cells were surface-biotinylated, and cell extract was prepared. Immunoprecipitation was done overnight using either TH-111 antibody or recombinant hCD155-lgG as indicated below the blot. The precipitated proteins were resolved by 10% SDS-PAGE under reducing conditions, and the bands were visualized following Western transfer applying streptavidin-alkaline phosphatase/nitro blue tetrazolium/5-bromo-4-chloro-3-indolyl phosphate. KG1 cells were used a source of endogenously expressed hCD96, whereas V1, V2, and ICAM-1 denote HEK293 cells transiently expressing hCD96V1, hCD96V2, and murine ICAM-1, respectively.



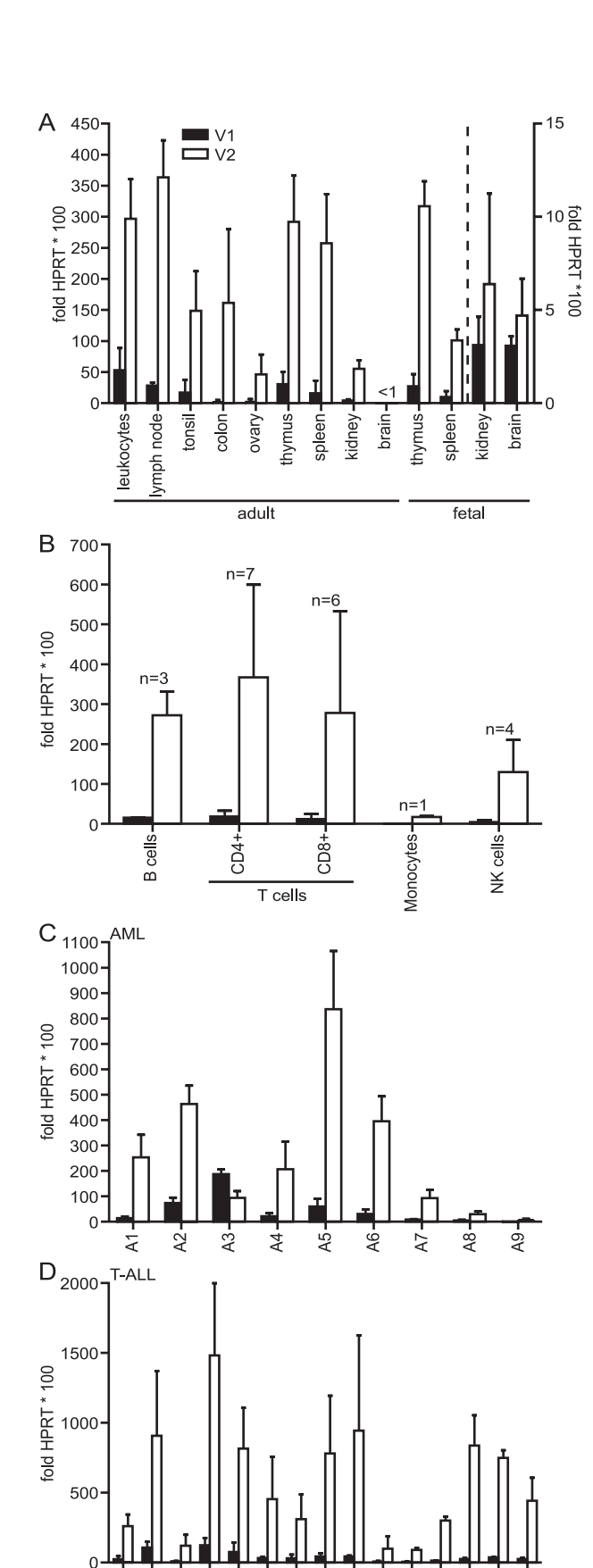


FIGURE 2. Determination of hCD96 expression by real time PCR. Primers specifically amplifying mRNA coding for hCD96V1 (V1) or hCD96V2 (V2) were used to determine the expression levels relative to that of the housekeeping gene hypoxanthine phosphoribosyl transferase. Shown are the results from at least two up to six independent experiments. Note that the dashed line in A

ည

of \sim 160 kDa. This confirms earlier observations (1) and indicates extensive post-translational modification as already shown for murine CD96 (5). Following cloning of the fulllength cDNA encoding hCD96V1 and hCD96V2, the sizes of the two variants were analyzed separately following transient expression in HEK293 cells, which are devoid of endogenous hCD96. A clear cut difference in size was not observed, even though hCD96V2 gave rise to a slightly faster migrating band. This also explains why the immunoprecipitate of biotinylated KG1 material appeared as a single band in the Western blot (Fig. 1F), although PCR indicated that both hCD96 variants are expressed by these cells (Fig. 1D).

We analyzed the expression pattern of the two human CD96 isoforms in various human organs with a special emphasis on lymphoid tissue. Real time PCR revealed considerable expression of CD96 in peripheral leukocytes, thymus, lymph nodes, tonsils, spleen, as well as colon and moderate levels in ovary and kidney (Fig. 2A). An hCD96-specific message could not be detected in prostate (not shown) and brain. Among fetal tissues, hCD96 was found to be expressed in thymus and spleen at levels comparable with the adult organs and to a considerably lesser extent in kidney and brain. Because we failed to detect hCD96 in adult brain, this may indicate that hCD96 is expressed exclusively during distinct developmental stages.

hCD96 was reported to be expressed on T cells, a subpopulation of B cells, and NK cells but not on monocytes and granulocytes. Therefore, white blood cells from healthy donors were isolated, sorted by flow cytometry, and/or magnetic bead separation (see "Experimental Procedures") and the mRNA levels representing the two hCD96 variants determined in CD19⁺ B cells, CD3⁺ CD4⁺ T cells, CD3⁺ CD8⁺ T cells, CD14⁺ monocytes, and CD3⁻ CD56⁺ NK cells (Fig. 2B). In all of the subsets studied, hCD96V2 predominated, although a considerable variation of the hCD96 levels between individual blood donors was observed, especially regarding their T cell subpopulations (see error bars in Fig. 2B).

Because hCD96 was identified as tumor marker expressed in T-ALL and AML (2, 3), it was of interest to test the hCD96 expression pattern in a panel of samples representing these types of leukemias (Fig. 2, C and D). Confirming earlier results, we observed a broad range of expression levels among both AML and T-ALL samples. However, in all of the T-ALL tumors analyzed, hCD96V2 represents the major hCD96 isoform to an extent as already seen for healthy T cells. In AML cells, the general expression level of CD96 seem more moderate when compared with T-ALL, even though also the AML panel is distinguished by a huge variability regarding the individual CD96 expression levels. In contrast to T-ALL, one AML sample (Fig. 2C, A3) displayed a marked switch in the isoform expression pattern usually observed with variant 1 predominating.

It has been reported that hCD96 protein levels increase several days following either allogenic or phytohemagglutinin-me-

separates the data for fetal kidney and the data for brain, for which another scale applies. B, amount of hCD96 variant specific RNA present in various blood cell subpopulations as indicated. n denotes the number of blood donors. C and D, hCD96 variants expressed by 9 AML (A1-A9) and 15 T-ALL (T1-T15) tumor samples.



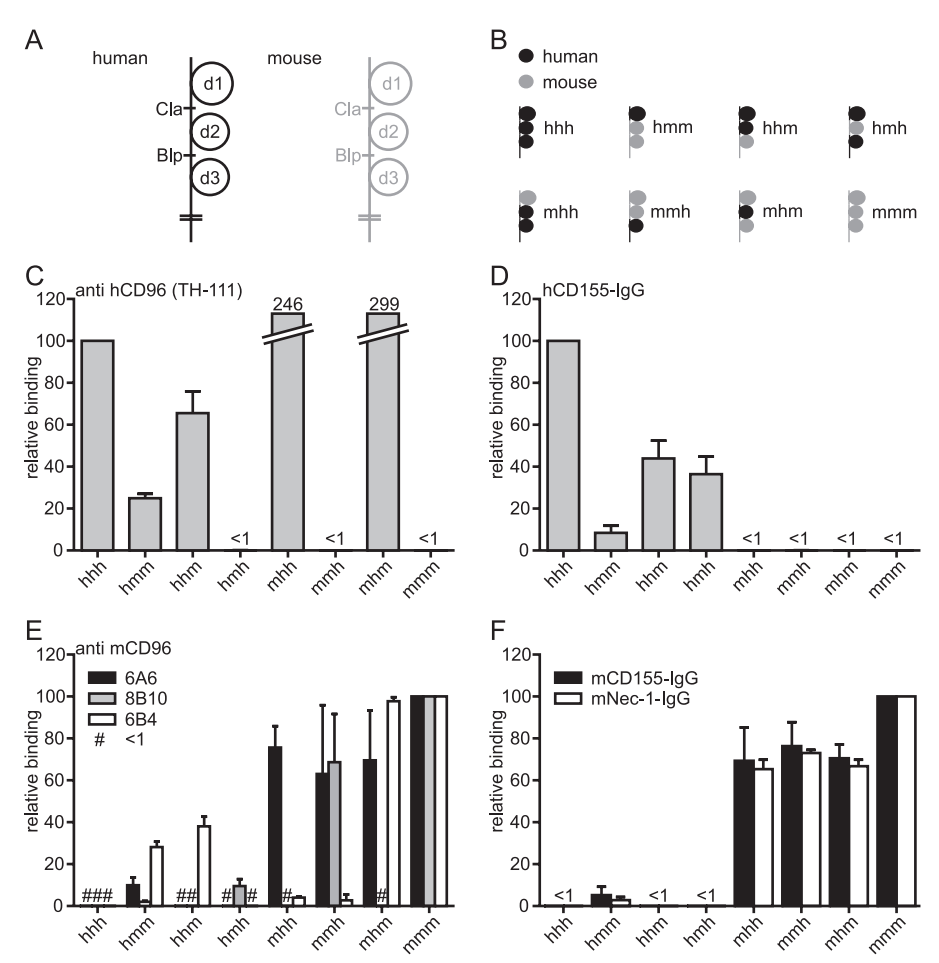


FIGURE 3. Composition of chimeric CD96 receptors and binding of monoclonal antibodies as well as recombinant proteins. *A*, by site-directed mutagenesis, recognition sites for the restriction enzymes Clal (domain 1/2 border) and Blpl (domain 2/3 border) were introduced into the wild type cDNAs coding for hCD96V2 and mCD96. *B*, schematic drawings of the chimeric receptors generated by domain exchange. *C–F*, the chimeric receptors were heterologously expressed by transfecting HEK293 cells along with a tenth of the amount of a green fluorescent protein expression plasmid to allow for gating on highly transfected cells. At least three independent experiments were performed. *C* and *D*, binding of anti-hCD96 mAb TH-111 or recombinant hCD155-hlgG1, respectively, to construct hhh was set to 100. *E* and *F*, binding of anti-mCD96 mAb 6A6, 8B19, 6B4, or recombinant mCD155-hlgG1, murine nectin-1-hlgG1 was set to 100.

diated stimulation, thereby coining the original name of CD96: Tactile (T cell activation, increased late expression) (1). To analyze whether the splicing of hCD96 pre-mRNA is influenced during T cell stimulation, peripheral T cells treated with phytohemagglutinin or anti-CD3 mAb OKT3 were studied. hCD96 protein expression was down-regulated within the first 2-3 days, but at later time points, a significant up-regulation was observed (not shown), thereby confirming earlier results (1). This particular kinetic of regulation was paralleled by the mRNA levels, although these declined earlier and to more pronounced degree. Again, the hCD96 variant specific pattern remained unchanged with hCD96V2 message predominating by a factor of ~ 10 at all time points investigated (not shown).

The First Ig-like Domain of CD96 Is Necessary for Binding to CD155—We next intended to determine the location of the binding epitopes on CD96 responsible for docking onto CD155 and nec-1. The finding that the CD155/CD96 interaction is not operating across the human/mouse species barrier (5) was exploited to construct chimeric human/mouse CD96 receptors based on hCD96V2 and mCD96. To achieve this, restrictions

sites were inserted into the domain 1/2 and domain 2/3 borders by sitedirected mutagenesis into each receptor cDNA (Fig. 3A). Next, chimeric receptors were cloned by domain exchange (Fig. 3) and named according to their species origin (Fig. 3B). For example, receptor mhh denotes a CD96 chimera where the first human domain was replaced by its murine equivalent. In all of the constructs, the species origin of the third domain also defines that of the S/T/P-rich stalk, the transmembrane region, and the cytoplasmic tail. The receptors were then transiently expressed in HEK293 cells, and binding of recombinant mouse or human CD155-hIgG1 proteins to them was monitored (Fig. 3, D and F). In addition, the binding of various anti-CD96 mAb to the chimeric receptors was tested (Fig. 3, C and E). As expected, the anti-hCD96 mAb TH-111 did not bind at all to the murine receptor. mAb TH-111 binding to chimeric receptors suggests that epitopes residing in the first two domains are recognized. Replacement of the second human domain substantially reduced (hmm) or eliminated binding (hmh, mmh), whereas that of the first domain surprisingly caused increased antibody binding (mhh, mhm). Exchange of the third human domain had only little impact on TH-111 binding. The hCD155 bind-

ing profile to the chimeric receptors indicates that the presence of the first human domain is obligatory for the interaction with the second and possibly third domain, modulating substantially the amplitude of binding activity (Fig. 3D). All of the chimeras of an hxx composition (where x denotes m or h) bound hCD155, albeit to a variable extent, whereas none of the mxx constructs was recognized. Inversely, mCD155 was capable to dock onto all receptors harboring a murine first domain with approximately equal efficiency and failed to bind those possessing a first domain of human origin (Fig. 3F).

Interestingly, murine CD96 and nectin-1 binding patterns were indistinguishable, and both interactions were insensitive to manipulations regarding downstream domains, indicating that the epitopes for both CD96 ligands are located exclusively in domain one. Human nectin-1 was also tested for binding, but this receptor did not to recognize hCD96, despite strongly binding to nectin-3, another known ligand (not shown). This suggests that the CD96/nec-1 interaction is not preserved between the two species (not shown).



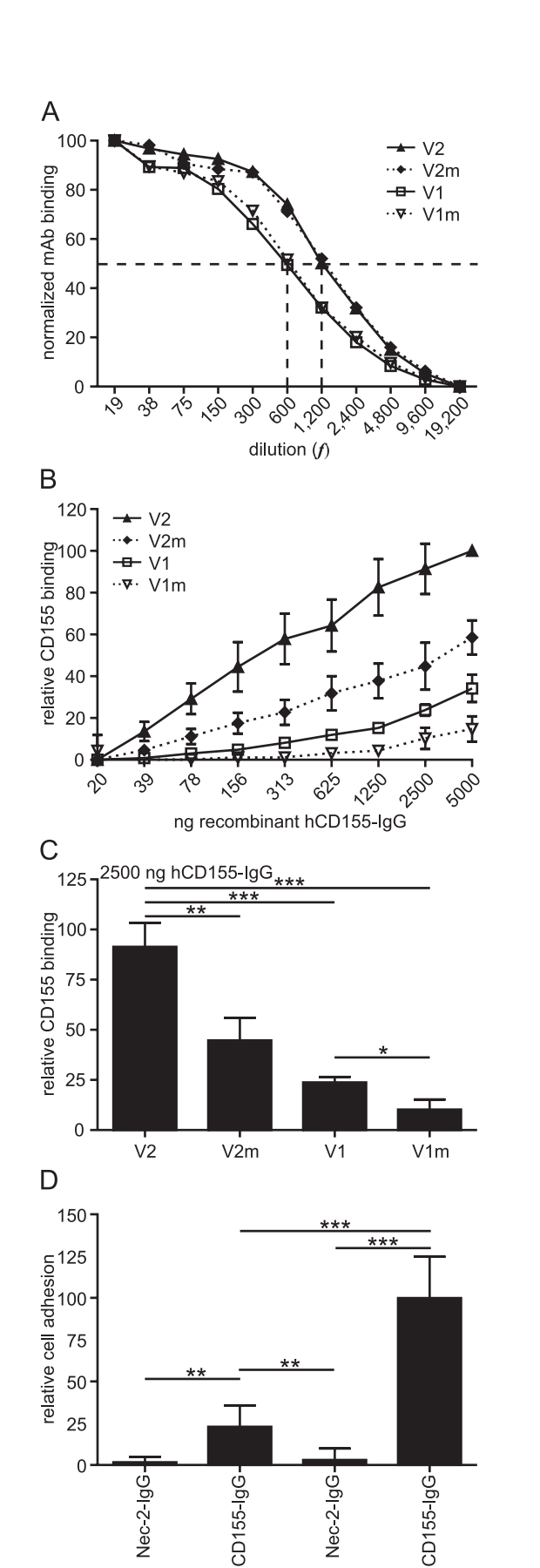


FIGURE 4. Binding of soluble ligands and cell adhesion assay. Alternative splicing and a mutation in domain three of hCD96 affect hCD155 binding. The binding of anti-hCD96 mAb TH-111 and recombinant hCD155-hlgG1 to

We made use of the chimeras to determine the binding patterns of the recently established anti-mCD96 mAb (clone 6A6 and 8B10) and also included a new clone (6B4). Three different patterns of mAb binding were obtained. Reminiscent to the recognition profiles of mCD155 and murine nectin-1, mAb 6A6 docked to domain one in a fashion that was largely independent of the composition of the downstream domains. Unlike that of mAb 6A6, mAb 6B4 binding is confined predominantly to chimeras possessing murine domain three because the exchange of this domain in all chimeras abolished mAb 6B4 attachment. In contrast, epitopes located in both domain 1 and 2, contribute to binding of mAb 8B10 as evidenced by the complete failure to bind either mhm or hmm.

The binding fingerprints of mAb 6A6 and recombinant mCD155-hIgG1 toward the chimeric CD96 receptors are identical, whereas that of mAb 8B10 diverges substantially (no binding to mhmCD96 and mhhCD96). This observation is in good agreement with the capacity of the anti-mCD96 mAb to block CD155 binding (5), because mAb 6A6 but not mAb 8B10 interfered completely with CD155 coupling.

Alternative Splicing of CD96 Influences Its Binding Capacity to CD155-Because the binding studies using the chimeric CD96 receptors revealed that the second hCD96 domain has an impact on CD155 binding, it is possible that the alternative splicing of this domain modulates the strength of the CD96/ CD155 interaction. Therefore, HEK293 cells transiently expressing either hCD96 isoform were incubated with serial dilutions of mAb TH-111 or recombinant hCD155-hIgG1 (Fig. 4). These titrations demonstrated that mAb TH-111 binding did not differ substantially between the two hCD96 variants (Fig. 4A). In contrast, titration of the recombinant CD155 protein uncovered drastic differences in binding. Although hCD96V2 binding reached a plateau when incubations were done in the presence of \sim 5–10 μg of recombinant hCD155 protein, that of hCD96V1 was distinguished by a graph, indicating that saturation binding would require unphysiologically high protein concentrations. Therefore, the differences in binding were depicted arbitrarily for an amount of 2.5 μ g of soluble binding partner present in the incubation mixes in Fig. 4C. We also cloned, expressed, and purified recombinant hCD96-IgG1 proteins representing the ectodomains of both isoforms and tested their binding to CD155 endogenously expressed by HEK293 cells. When titrating both recombinant hCD96 proteins, it was evident that the hCD155/hCD96V1 interaction is similarly less pronounced when compared with that between hCD155 and hCD96V2 as already observed for the inverse

receptors hCD96V1 (V1) and hCD96V2 (V2) or their T280M mutant form (V1m, and V2m, respectively) was analyzed in detail by titrating mAb TH-111 or hCD155-hlgG1. For calculations see "Experimental Procedures." A, binding was recorded using $\sim 2 \times 10^5$ transfected HEK293 cells/indicated data point. B, in parallel binding studies, recombinant hCD155-hlgG protein was used. C, summary of three independent experiments. Shown are the binding efficiencies when $2.5 \mu g$ recombinant protein was applied. D, cell adhesion assay. Raji cells transiently expressing hCD96V1 (V1) or hCD96V2 (V2) were allowed to bind to 1 μg of plastic coated murine Nec-2-lgG (control) or CD155-hlgG per 96-well for 90 min, and the wells were washed twice before the attached cells were quantitated as described under "Experimental Procedures." Binding of hCD96V2 expressing Raji cells to CD155-hlgG was set to 100%. The results from four experiments are shown. *, p < 0.05; **, p < 0.01; ***, p < 0.001.



V2

V1

setup (not shown). mAb D171 shown earlier to block binding of poliovirus to CD155 (15) also prevented that of CD96 (not shown) demonstrating that (i) CD155 represented the only binding option for recombinant hCD96 protein on the surface of the cells and ii) most likely the first domain of CD155 is involved in CD96 recognition because virus docking occurs via contacting epitopes located in the outermost V-like domain of CD155 (16).

To study the adhesive capacities of the hCD96 variants separately in a cellular context, Raji cells, a human B cell tumor line lacking endogenous hCD96, were transiently transfected with expression vectors coding for hCD96-EYFP fusion receptors. In this setup, the C-terminally tagged receptor did not differ in their cytosolic composition yet allowed for a direct monitoring of their expression levels by flow cytometry. When Raji cells transiently expressing equal amounts of the hCD96 variants (supplemental Fig. S1) were allowed to attach to plate-bound recombinant hCD155-IgG protein, similar differences in the adhesive properties were observed as already found for the soluble ligands (Fig. 4D). The amount of recombinant hCD155-IgG protein coated to the plate was close to maximum binding capacity (1 µg per96-well) because a density corresponding to less than 250 ng did not evoke attachment of hCD96V1-expressing cells. Thus, a cooperative binding of cell expressed hCD96V1 to a dense network of fixed hCD155 ligand could not compensate a pronounced weaker attachment capacity of this variant when compared with the strong binding elicited by variant 2. The firm adhesion mediated by the latter may also explain our observation that Raji cells expressing hCD96V2 (but not variant 1) exerted a conspicuous tendency to develop long dendritic protrusions upon attachment (see supplemental Fig. S1).

A Naturally Occurring Point Mutation in Domain 3 of hCD96 Impairs Binding to CD155—It was speculated recently that genetic abnormalities in the human CD96 locus may relate to a form of the C syndrome (Opitz Trigonocephaly) (8). A balanced chromosomal translocation, t(3;18)(q13.13;q12.1), was found to disrupt the CD96 gene in one case, whereas in another, a mis-sense mutation affecting domain three of hCD96 (T280M) was identified. Cells heterologously expressing wild type hCD96 or the mutated version displayed profound differences in their adhesive potential during the early stages of contact with the solid matrix of the culture plate. Therefore, the T280M mutation was introduced into both hCD96 variants generating hCD96V1m and hCD96V2m, and their binding capacity toward mAb TH-111 as well as soluble recombinant hCD155 was tested as outlined above (Fig. 4). Titrations revealed that mAb TH-111 binding to both CD96 isoforms is unaffected by the T280M mutation (Fig. 4A). In contrast, the capability of both hCD96 isoforms regarding their binding to hCD155 is severely hampered (Fig. 4B). Indeed, hCD96V1m/CD155 complex formation could only be detected at the highest concentrations of recombinant hCD155 protein applied (Fig. 4C), confirming that this particular domain three mutation has an impact on the adhesive capacity of hCD96. Along with the finding that variant 1 constitutes a considerable amount of the hCD96 message in fetal brain, the T280M mutation may elicit profound adhesive deficiencies for those neuronal cells

depending on CD96 function. Developing neurons migrate, a process requiring recurrent adhesion to and detachment from extracellular matrix or cellular scaffolds, whereas these cells may be particularly prone to defects in their adhesion receptor repertoire. It will be interesting to identify the cell type expressing CD96 in fetal brain or to generate a CD96-deficient mouse to learn more about the role of this receptor in developmental processes.

DISCUSSION

CD96 function(s) are poorly understood even if indirect evidence suggests that it represents an adhesion receptor involved in brain development as well as in immunologically relevant processes (see Introduction). The latter is substantiated by the expression of CD96 on T as well as on NK cells (Refs. 4 and 5 and this report). Apart from T and NK cells (4), little is known regarding hCD96 expression in other cell types or tissues, especially in the brain (8). Therefore, we quantitated the expression of hCD96 in several tissues and found substantial mRNA levels in all primary and secondary lymphoid organs investigated. In contrast, only a moderate expression was observed in nonlymphoid tissues such as ovary and kidney. When comparing fetal organs with their adult counterparts, the degree of hCD96 expression did not differ substantially in thymus and to an only moderate extent in spleen. In contrast, hCD96 mRNA is much more abundant in adult kidney, but it appears that this increase in hCD96 expression is caused predominantly by an elevated synthesis of hCD96V2 mRNA. Vice versa, little hCD96 specific mRNA was observed in fetal brain comparable with that observed in fetal kidney, but hCD96 message was undetectable in the adult organ. Moreover, the results suggest that variant 1 contributes much more to the CD96 mediated adhesiveness in fetal kidney and brain when compared with any other organ.

A more detailed analysis of white blood cell subsets revealed that the level of hCD96 expressed by both CD4⁺ and CD8⁺ T cells varies substantially depending on the individual blood donor. However, a vast excess of variant 2-specific message over that coding for variant 1 represented a constant feature of the hCD96 expression pattern regardless of its expression strength in all individuals tested. This was already evident from the analyses of pooled tissue samples discussed above and extended to the results obtained when tumor samples from patients suffering from AML or T-ALL were investigated. However, in one particular case, the AML sample A3 (Fig. 2C), a noticeable divergence was observed with the level of variant 1-specific RNA exceeding that of variant 2. Whether both the expression level per se or the reversed ratio regarding variant 1 and 2 expression can be exploited as diagnostic tool must await further studies including considerably higher sample numbers.

Human but not mouse CD96 can be expressed in two isoforms based on differential splicing. The assumed function of hCD96 as a NK receptor relates to its specific binding to CD155 (4). Like hCD96, hCD155 is also known to exist in various isoforms (four splice variants), whereas only one type of mRNA codes for mCD155 (17–19). However, alternative splicing of hCD155 pre-mRNA does not involve the Ig-like domains, whereas the capacity of the receptor to interact with its ligands is identical for all isoforms. In contrast, alternative



splicing of the hCD96 pre mRNA allows for the synthesis of receptors differing in the Ig-specific fold of the second Ig-

The function of adhesion receptors is critically defined by the spectrum of ligands they are recognizing. Therefore, we analyzed the binding properties of human as well as murine CD96 in more detail with respect to the domains mediating the interaction with CD155 and nec-1. Dissecting the three Ig-like domains by generating chimeric human/murine CD96 receptors revealed that binding epitopes contacting the ligand reside in domain one, the most membrane-distal domain of the molecule that is supposed to be easily accessible even for bulky ligands. The absolute requirement for the first domain in ligand docking is illustrated by the finding that all receptors lacking it invariantly lost their CD155 binding capacity independent of the species origin. However, human and murine CD96 differ in several other aspects. First, the human receptor does not interact with nec-1, and second, CD96 binding to CD155 and nec-1 is almost independent of domain two (and three) in mouse. In contrast, hCD155 binding strength is sensitive to the molecular composition of the downstream domains (see also below). It is currently not known whether the artificial composition of human and murine domains interferes with correct folding of the chimeric receptors thus giving rise to a highly variable binding of hCD155. However, such indirect effects should also hamper mCD155 binding even if its binding is largely restricted to the first domain of mCD96. In addition, the finding that a naturally occurring splice variant profoundly modulates binding favors an involvement of the downstream domains in the adhesiveness of hCD96. It is remarkable that both features concur in human but not mouse dependence of binding strength on downstream domains and alternative splicing. Whether the contribution of the second/third domain toward hCD155 binding is direct or indirect in nature remains unclear, but it is interesting to note that the alternative splicing occurs under preservation not only of the open reading frame but also of the Ig-like core folding pattern. It is tempting to speculate that the differing Ig fold causes an alternative presentation of the first domain with respect to the other domains of hCD96, thereby impeding the access to essential amino acids required for ligand docking in case of variant one. Remarkably, NKp30 is also known to occur in two splice variants giving rise to either a V-like or a C-like Ig-domain (20). Even though the functional consequences of this alternative splicing remain obscure, NKp30 represents a NK receptor, and the conspicuous similarities between CD96 and NKp30 extend to the observation that both receptors are expressed in fetal brain (21). Although we could attest only a rather low expression level in fetal brain, in the absence of detectable hCD96 expression the adult organ would correlate with a putative function of this receptor in the development of the central nervous system.

Therefore, it was of interest to investigate the impact on the adhesiveness of a recently published point mutation of hCD96 that maps to the third Ig-like domain (T280M) and that occurred in a patient suffering from C syndrome (Opitz trigonocephaly). In contrast to hCD155 binding, that of anti-hCD96 mAb TH-111 is not affected by T280M. This is in line with the finding that epitopes recognized by mAb TH-111 are located in

domain 1 and 2 with domain 3 exerting only little impact on binding. This is illustrated by the observation that TH-111 bound with almost wild type characteristics to receptor hhm, whereas that of CD155 remained at a lower level. In contrast, TH-111 binding to hmh was undetectable, whereas this chimera preserved a considerable capacity to interact with CD155. The latter finding suggests that also the third human CD96 domain is critically involved in ligand binding. Nevertheless, Kaname et al. (8) reported that the T280M exchange reduced unspecific adhesiveness to plastic substrate, suggesting that this mutation triggers a conformational alteration of the domains with respect to each other or to neighboring attachment receptors, thus resembling the scenario as discussed above for the hCD96 splice variants. The threonine affected by the mutation maps to the N-terminal end of the putative A' strand of the third domain located in close proximity to the S/T/P rich stalk, which emanates from the neighboring G strand of the same domain. The human sequence surrounding Thr²⁸⁰ is: 275 VENNSTDVL 283 (Fig. 1*C*). The murine sequence is closely similar: 256VENSTMDVL264. These sequences and their comparison reveal that the human AA' region is equipped with a double N-linked glycosylation site (NNST), whereas the murine strand harbors only one such site.

Although glycosylation at these sites remains speculative, the mutation from a hydrophilic polar to a more nonpolar hydrophobic residue may change the surface characteristics of the N-terminal part of the domain. Several variable Ig domains involved in interactions with other proteins or with as yet undefined ligands show variability in this area (see Ref. 22 for DSCAM in insects and Ref. 23 for V region-containing chitinbinding proteins in amphioxus), and changes in this region indeed can be expected to result in modifications of binding capacity. However, in the case of CD96 the binding interface seems to depend on the nonmutated first V domain essentially (see above). Yet, an extra modification, brought in by the mutation, might affect either the orientation of the molecule or perhaps the interaction with a coreceptor. Interestingly, because the threonine in the human sequence is (already) replaced by a methionine in mouse, the T280M mutation converts the topology of the human AA' strand into a murine-like conformation. Along with the observation that the murine CD155 binding to CD96 is rather insensitive to structural features beyond the first domain, whereas the corresponding human interaction relies on downstream domains, we speculate that the murinization of the distal third Ig-like domain withdraws the (conformational) support of the lower domains required in human for full binding. These differences would also help explain why the CD155/ CD96 interactions are species-specific, i.e. murine CD155 can interact only with murine CD96 but not with human CD96 and vice versa, even if the key amino acids required for binding would otherwise be similar or identical.

In this report, we demonstrated that CD96 engages interactions in trans via epitopes mapping to the most N-terminally located first Ig-like domain. However, the molecular terms influencing binding are different between man and mouse as evidenced by the interaction of CD96 with CD155. In contrast to mice, the adhesive properties of human CD96 are modulated by characteristics of downstream domains that most likely do



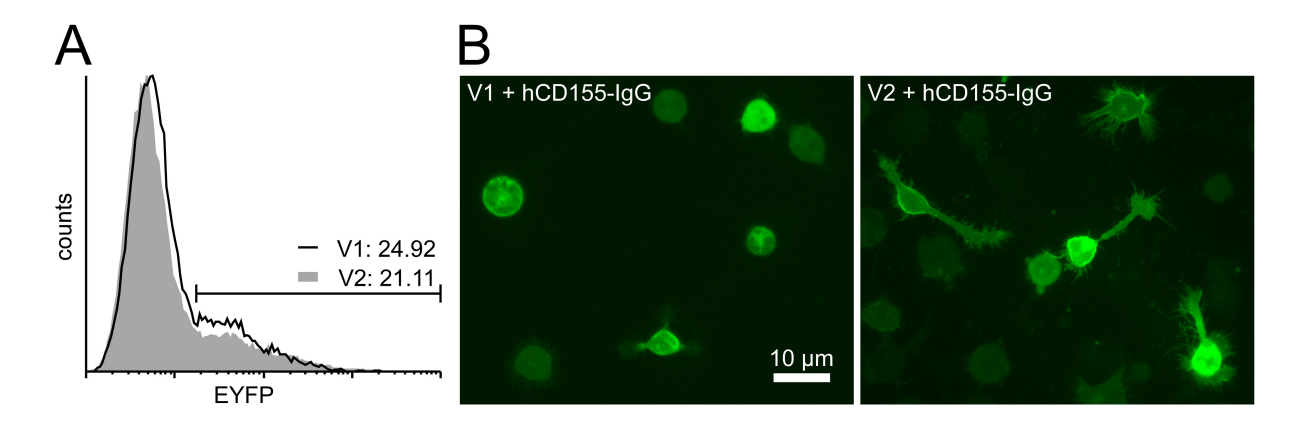
not contact ligand by themselves but rather warrant optimal docking conditions by providing conformational assistance. This also corroborates that the interaction parameters developed along different evolutionary constraints in man and mouse: a robust binding to CD155 in mouse and a more diversified interaction with CD155 that is subject to modulation by splicing conditions in human. The emergence of these differences was also fostered by the rapid evolutionary diversification of both CD96 and CD155, as reflected by the low degree of amino acid sequence conservation (5). Yet the interaction between the receptors was preserved substantiating its biological significance. Taken together, the CD96 function(s) apparently overlap between the species, but others may be unique, e.g. those driven by the murine CD96/nectin-1 interaction that is absent in human. Vice versa, only the human cytoplasmic tail contains a YXXM motif, a potential SH2 domain-binding site for the p85 subunit of the pl3 kinase frequently encountered in coreceptors of the Ig superfamily and involved in signaling (24). It will be instructive to study the signaling mediated by human and murine CD96 in more detail because their short transmembrane and cytoplasmic tails share several other conserved features such as an ITIM resembling motif (IXYXXI). A cysteine residue located in the trans membrane domain along with positively charged amino acids at the transmembrane/cytoplasmic interface probably serve as a binding site for Src-related kinases (25). In addition, a proline-rich region in the intracellular tail could allow signaling/adaptor proteins possessing SH3 domains to dock onto CD96 (26).

Acknowledgments—We thank Dr. M. Ballmaier and Ch. Reimer for cell sorting, Dr. M. Peipp for help in providing antibody TH-111, and Dr. M. Stanulla and Dr. J. Krauter for providing cDNA tumor samples representing T-ALL and AML, respectively.

REFERENCES

- Wang, P. L., O'Farrell, S., Clayberger, C., and Krensky, A. M. (1992) J. Immunol. 148, 2600 –2608
- Gramatzki, M., Ludwig, W. D., Burger, R., Moos, P., Rohwer, P., Grunert, C., Sendler, A., Kalden, J. R., Andreesen, R., Henschke, F., and Moldenhauer, G. (1998) Exp. Hematol. 26, 1209–1214
- Hosen, N., Park, C. Y., Tatsumi, N., Oji, Y., Sugiyama, H., Gramatzki, M., Krensky, A. M., and Weissman, I. L. (2007) *Proc. Natl. Acad. Sci. U. S. A.* 104, 11008 –11013
- 4. Fuchs, A., Cella, M., Giurisato, E., Shaw, A. S., and Colonna, M. (2004)

- J. Immunol. 172, 3994-3998
- Seth, S., Maier, M. K., Qiu, Q., Ravens, I., Kremmer, E., Forster, R., and Bernhardt, G. (2007) Biochem. Biophys. Res. Commun. 364, 959 –965
- Inagaki, M., Irie, K., Ishizaki, H., Tanaka-Okamoto, M., Morimoto, K., Inoue, E., Ohtsuka, T., Miyoshi, J., and Takai, Y. (2005) *Development* 132, 1525–1537
- Suzuki, K., Hu, D., Bustos, T., Zlotogora, J., Richieri-Costa, A., Helms, J. A., and Spritz, R. A. (2000) Nat. Genet. 25, 427–430
- 8. Kaname, T., Yanagi, K., Chinen, Y., Makita, Y., Okamoto, N., Maehara, H., Owan, I., Kanaya, F., Kubota, Y., Oike, Y., Yamamoto, T., Kurosawa, K., Fukushima, Y., Bohring, A., Opitz, J. M., Yoshiura, K., Niikawa, N., and Naritomi, K. (2007) *Am. J. Hum. Genet.* 81, 835–841
- Takai, Y., Irie, K., Shimizu, K., Sakisaka, T., and Ikeda, W. (2003) Cancer Sci. 94, 655–667
- Du Pasquier, L., Zucchetti, I., and De Santis, R. (2004) *Immunol. Rev.* 198, 233–248
- Bottino, C., Castriconi, R., Pende, D., Rivera, P., Nanni, M., Carnemolla, B., Cantoni, C., Grassi, J., Marcenaro, S., Reymond, N., Vitale, M., Moretta, L., Lopez, M., and Moretta, A. (2003) J. Exp. Med. 198, 557–567
- Maier, M. K., Seth, S., Czeloth, N., Qiu, Q., Ravens, I., Kremmer, E., Ebel, M., Muller, W., Pabst, O., Forster, R., and Bernhardt, G. (2007) Eur. J. Immunol. 37, 2214–2225
- Cario, G., Izraeli, S., Teichert, A., Rhein, P., Skokowa, J., Moricke, A., Zimmermann, M., Schrauder, A., Karawajew, L., Ludwig, W. D., Welte, K., Schunemann, H. J., Schlegelberger, B., Schrappe, M., and Stanulla, M. (2007) J. Clin. Oncol. 25, 4813–4820
- Czeloth, N., Bernhardt, G., Hofmann, F., Genth, H., and Forster, R. (2005)
 J. Immunol. 175, 2960 –2967
- Nobis, P., Zibirre, R., Meyer, G., Kühne, J., Warnecke, G., and Koch, G. (1985) J. Gen. Virol. 66, 2563–2569
- Bernhardt, G., Harber, J. J., Zibert, A., deCrombrugghe, M., and Wimmer,
 E. (1994) Virology 203, 344 356
- 17. Ravens, I., Seth, S., Forster, R., and Bernhardt, G. (2003) *Biochem. Biophys. Res. Commun.* **312**, 1364–1371
- Mendelsohn, C. L., Wimmer, E., and Racaniello, V. R. (1989) Cell 56, 855–865
- 19. Koike, S., Horie, H., Ise, I., Okitsu, A., Yoshida, M., Iizuka, N., Takeuchi, K., Takegami, T., and Nomoto, A. (1990) *EMBO J.* **9,** 3217–3224
- 20. Neville, M. J., and Campbell, R. D. (1999) J. Immunol. 162, 4745-4754
- 21. Hollyoake, M., Campbell, R. D., and Aguado, B. (2005) *Mol. Biol. Evol.* 22, 1661–1672
- Watson, F. L., Puttmann-Holgado, R., Thomas, F., Lamar, D. L., Hughes, M., Kondo, M., Rebel, V. I., and Schmucker, D. (2005) Science 309, 1874–1878
- Cannon, J. P., Haire, R. N., Schnitker, N., Mueller, M. G., and Litman, G. W. (2004) Curr. Biol. 14, R465–466
- 24. Chambers, C. A. (2001) Trends Immunol. 22, 217-223
- 25. Rozsnyay, Z. (1999) Immunol. Lett. 68, 101-108
- 26. Kay, B. K., Williamson, M. P., and Sudol, M. (2000) FASEB J. 14, 231–241



Supplementary figure 1: Raji cells were transfected with a construct encoding for either CD96V1 or CD96V2 fused to EYFP. A: Flow cytometric control of the transfection efficacy for V1 (solid line) and V2 (shaded area). Given are the percentages of EYFP⁺ cells. B: Tracking of transfected Raji cells by flourescence microscopy. Adhesion of the cells to cover slips coated with recombinant hCD155-IgG was monitored. The cellular distribution of the EYFP signal indicates efficient surface presentation of CD96. Morphological changes in terms of cell protrusions are most prominent among V2 transfected cells and were rarely observed in V1 transfected cells. No surface adhesion of transfected Raji cells could be detected when using mCD112-IgG control protein.

CD96 Interaction with CD155 via Its First Ig-like Domain Is Modulated by Alternative Splicing or Mutations in Distal Ig-like Domains

Dorothee Meyer, Sebastian Seth, Jana Albrecht, Michael K. Maier, Louis du Pasquier, Inga Ravens, Lutz Dreyer, Renate Burger, Martin Gramatzki, Reinhard Schwinzer, Elisabeth Kremmer, Reinhold Foerster and Günter Bernhardt

J. Biol. Chem. 2009, 284:2235-2244. doi: 10.1074/jbc.M807698200 originally published online December 4, 2008

Access the most updated version of this article at doi: 10.1074/jbc.M807698200

Alerts:

- When this article is cited
- When a correction for this article is posted

Click here to choose from all of JBC's e-mail alerts

Supplemental material:

http://www.jbc.org/content/suppl/2008/12/06/M807698200.DC1.html

This article cites 26 references, 11 of which can be accessed free at http://www.jbc.org/content/284/4/2235.full.html#ref-list-1